Investigation of Channel Spatial Diversity for Dual-link Cooperative Communications in WBAN

Lingfeng Liu*†, Vaibhav Bhatnagar*, Cristina Garcia Robles*,
Philippe De Doncker†, Luc Vandendorpe*, Claude Oestges*
* ICTEAM, Université catholique de Louvain (UCL)
3 Place du Levant, 1348 Louvain-la-Neuve, Belgium
† OPERA, Université libre de Bruxelles (ULB)
CP 194/5, Avenue F. D. Roosevelt 50, B-1050 Bruxelles, Belgium
lingfeng.liu@uclouvain.be, vaibhav.bhatnagar@uclouvain.be, cristina.garcia@student.uclouvain.be
pdedonck@ulb.ac.be, luc.vandendorpe@uclouvain.be, claude.oestges@uclouvain.be

***Abstract*—In this work, we investigate the spatial diversity gain offered by on-body channels in indoor environments. Narrowband on-body channel measurements are conducted in a dual-link topology, to cover various scenarios with different link geometries and body movements. Cooperative dual-link communications with equal-power allocation scheme are evaluated based on the channel measurements. The simulated bit-error-rate (BER) of the cooperative dual-link is compared with the single-link performance. The results highlight the performance of the cooperative scheme for uncorrelated channels with significant fading variance and close pathloss level. In such cases, spatial diversity effectively improves the quality and BER of on-body communications.**

I. Introduction

Wireless body area networks (WBANs) are bringing significant innovation in medical applications to enable long-term wireless monitoring of the patients. This technology resorts to short range communications between compact sensors/units that are either implanted, worn, or placed in the vicinity of the human body to detect and convey critical biomedical signals [1]. Practical WBANs applications are challenged by the strict requirements in power consumption and transmission quality. Frameworks like ZigBee/IEEE 802.15.4 [2], [3] propose to use one or more body-worn data sinks to collect the signals from the sensors for processing and transmitting to the outside networks. Such transmissions occurring on the surface of the body (hence, the name on-body communications), are deeply impacted by the scattering effects from both the body and the environment. In particular, on-body channels are characterized by: (1) pathloss levels which are high even over short distances, and sensitive to the polarization and the distribution of the channels [4]; (2) deep fading in time and spatial domains due to the movements of the body and the multi-path effects from the environment [4]–[7]. As a result, large fluctuations of the signal-to-noise ratio (SNR) are anticipated in realistic WBAN systems despite short inter-node distance, resulting in link outages which are difficult to resolve with common communication technologies.

A promising solution to overcome the uncertainty of on-body channels is to deploy cooperative multi-link technologies to exploit the spatial diversity from multiple channels in order to mitigate the deep fading in a single on-body channel, as studied in [8]. The efficiency of a cooperation scheme is however limited by the design of the sensors, while its performance is highly dependent on the channel properties, such as the level of pathloss, the variation of the channel fading, and the correlation between the channels. Particularly, the dynamic propagation environment from one posture to another posture changes so significantly that the BER benefits from a static cooperation scheme could easily get lost. This calls for a detailed characterization of on-body channels in both time and spatial domains.

In this paper, we report on narrowband on-body channels measurements using a dual-link topology in realistic indoor environments. We characterize the time-variant channel fading in each scenario, with different link geometries and body movements. A cooperative dual-link with a simple, equal-power allocation scheme is simulated based on the channel measurements. The performance of this cooperation scheme is evaluated via the bit-error-rate (BER) gain achieved in the dual-link configuration and compared with the single-link performance. Relationships between the BER gain and the channel properties are also analyzed.

The paper is organized as follows, Section II describes the context of the measurements; Section III presents the radio channel characterization; Section IV evaluates the diversity gain in the cooperative dual-link; and at last, Section V summarizes our analysis.

II. Measurement Framework

The goal of this work is to measure on-body channels in a dual-link topology with one common transmitter (Tx) and two receivers (Rx). Narrowband measurements were conducted at 2.47 GHz over a female volunteer. Five scenarios were investigated with different link geometries, as described in Fig. 1. The link geometries correspond to regions of medical monitoring, like the chest, wrist, legs, and arms. Measurements in each scenario include three different cases of body movements: sleeping in a small room simulating the hospital environment, shown in Fig. 2(a), a series of sit-stand motions in an indoor environment, shown in Fig. 2(b), and a slow walking motion in

TABLE I
MEASUREMENT SETUP AND BODY INFORMATION

Input power	5 dBm	Frequency	2.47 GHz
IF bandwidth	1 kHz	Sampling rate	1 ms
Measurement length	10 s	Body height/weight	170 cm/65 kg
Waist perimeter	77 cm	Hip perimeter	87 cm

the same indoor environment. Each measurement in a specific case is 10 second long.

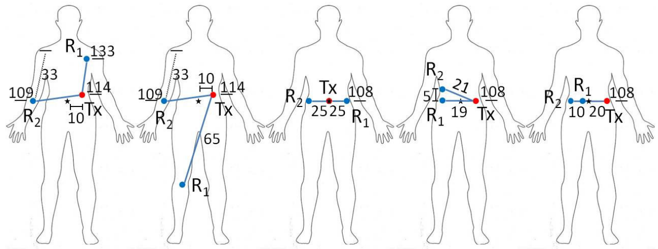

Fig. 1. Five on-body propagation scenarios, labeled as scenarios 1, 2, 3, 4, 5, from left to right: Tx represents the transmitter, and R_1 and R_2 represent the receivers for channels 1 and 2 (positions of the antennas are measured in centimeters, and their height is measured from the ground)

(a) Sleeping case

(b) Sit-stand and walking cases

Fig. 2. Motion scenarios

The channels were measured by the transmission S-parameters using an Agilent PNA-X N5242A vector network analyzer (VNA). The detailed setup of the measurement is provided in Table I.

Three small-sized tangentially polarized SMT-3TO10M-A Skycross antennas were directly attached on the skin. The efficiency of the antennas is evaluated through the return loss, i.e. S_{11} parameter. The average return-loss of both the Tx and

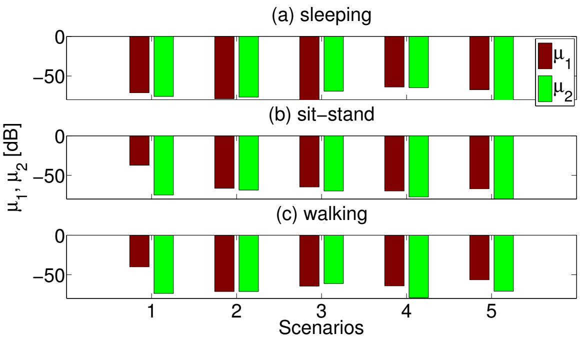

Fig. 3. Comparison of mean, μ, of the fading amplitudes (on dB scale) for channels 1 and 2

Rx was found to remain at a tolerable level (-9 dB in sleeping cases, -10.2 dB in sit-stand cases, and -16.4 dB in walking cases).

III. CHANNEL CHARACTERIZATION

The statistics of the time-variant channel fading amplitude are extracted for each motion mode in each link scenario. Fig. 3 and Fig. 4 present the mean, μ, and the standard deviation (std), σ, of the fading amplitude on dB scale respectively. In most measurements, channels 1 and 2 have different pathloss levels. The largest pathloss difference between both channels is found to be 37.6 dB (in sit-stand case, scenario 1). On the contrary, channels in the sit-stand and walking cases in scenarios 2 and 3 have closer pathloss. For a given scenario, the pathloss can also change over different cases due to the change of the postures and strong reflections from the surrounding objects. This can be observed for channel 1, comparing the sleeping and sit-stand cases in scenario 1. The temporal channel fading is caused by the dynamic scattering from the body movements and the multi-paths effect from the environment. It is natural to observe a small variation of the channel fading in sleeping cases in Fig. 4, since the body was not moving and the environment was quite stationary. It is also interesting to find that channel fading in sit-stand cases exhibits larger variations than in walking cases. This is anticipated since the change of the posture from sit to stand is quite significant, which will bring larger variation of the body scattering. Generally, the pathloss in realistic environments results from the combination of the link geometry, polarization, body scattering, and antenna gain.

The distribution of the fading amplitude (in linear scale) is now investigated. The maximum-likelihood estimator (MLE) is applied to estimate the following distributions: (1) Lognormal; (2) Gamma; (3) Nakagami; (4) Rayleigh; (5) Normal; (6) Weibull; (7) Exponential. The estimation results are evaluated by comparing the mean square error (MSE). The average MSE over all cases are presented in Fig. 5. It is clear that the Rayleigh distribution, although commonly considered for indoor propagation, does not fit the on-body channel fading. The Lognormal, Gamma, and Weibull distributions show close performance with the lowest MSEs.

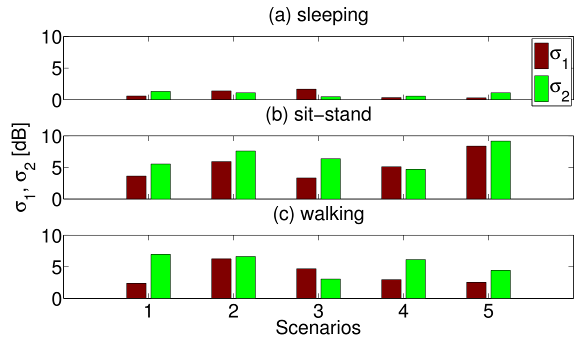

Fig. 4. Comparison of std, σ, of the fading amplitudes (on dB scale) for channels 1 and 2

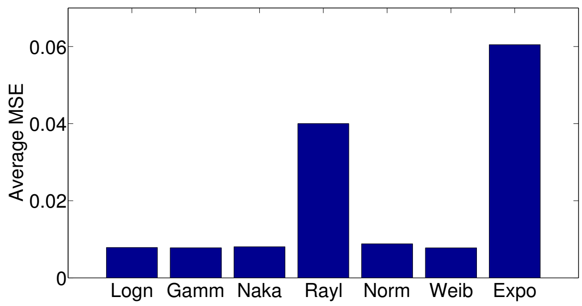

Fig. 5. Average MSE of estimated fading distributions

The correlation between channels 1 and 2 is investigated via the correlation coefficient, ρ_{12} of their fading amplitudes on dB scale (as the fading amplitudes have been found to be lognormally distributed by Fig. 5), which are presented in Fig. 6. De-correlations between the channels are widely found in sleeping, sit-stand, and walking cases. In some scenarios, a higher channel correlation is found in sit-stand cases. This is probably due to the significant scattering effect during large changes of the body posture that dominates the time-variation of the channels. Anti-correlation between the channels are found in the walking case, scenario 2. Similar observations were also found in other studies [9].

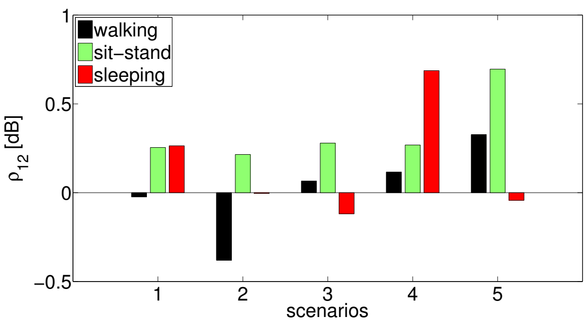

Fig. 6. Correlation coefficients of the fading amplitudes (on dB scale) of channels 1 and 2

IV. Diversity Analysis

We consider the quadrature phase-shift keying (QPSK) modulation, suggested in IEEE 802.15.4, to carry out the BER analysis for both single-link and dual-link communications. The BER of QPSK is a Q-function of the SNR [10]–[12]. The average BER is then expressed as:

$$\mathrm{BER}(\mathrm{SNR}_{\mathrm{Tx}}) = \sum_{n=1}^{N} \frac{Q(\sqrt{2|h(n)|^2 \mathrm{SNR}_{\mathrm{Tx}}})}{N}, \tag{1}$$

where the $\mathrm{SNR}_{\mathrm{Tx}}$ is the SNR evaluated at the transmit side, $|h(n)|^2$ is the channel gain at time instant n, and N is the total number of temporal samples. To analyze the channel diversity, the Q-function in Eq. 1 takes the SNR at the receive side as the input to normalize the channel gain. The BER in both dual-link and single-link schemes are also compared with the reference BER in additive white Gaussian noise (AWGN) channels.

The channel spatial diversity can be exploited for cooperative dual-link through e.g. the Alamouti code [13]. In this paper, we consider an equal-power allocation scheme, as suggested by [14], to reduce the complexity in practical cooperative systems. To evaluate the BER in the dual-link configuration, the dual-link SNR at the receive side is defined as [15]:

$$\mathrm{SNR}_{\mathrm{Rx},D} = \mathrm{SNR}_{\mathrm{Tx}} \frac{|h_1|^2 + |h_2|^2}{2}, \tag{2}$$

where $|h_1|^2$ and $|h_2|^2$ represent channels 1 and 2. In (2), the component $(|h_1|^2 + |h_2|^2)/2$ is treated as the synthesized channel for the dual-link.

The equal-power allocation scheme is applicable when the pathloss levels of both channels are close. By contrast, when channel 1 is sensibly above channel 2, e.g. in the sit-stand case in scenario 1 as depicted in Fig. 7(a), allocating half transmit power to each channel will only cause a 3 dB decrease of the SNR of the dual-link without mitigating the fading of channel 1. As a result, the simulated dual-link BER in Fig. 7(b) does not get benefits from channel diversity. Under this situation, it is suggested to only use the best channel rather than Alamouti combining.

On the other hand, it is obvious that cooperative communications will not get benefits from channel diversity if the single channels are already quite flat. From Fig. 4, one example can be found in the sleeping case, scenario 4, as shown in Fig. 8. The BERs achieved in either single-link or dual-link schemes are quite close to the BER achieved in AWGN channels, meaning that no diversity gain can be achieved when there is no significant fading in the single channels.

Fig. 9 and Fig. 10 present two measurements for which channels 1 and 2 exhibit close pathloss levels, yet with significant fading. In both measurements, channels 1 and 2 are uncorrelated or anti-correlated as shown in Fig. 6. Both cases show significant diversity gains in the BER comparison in Fig. 9(b) and Fig. 10(b). From the synthesized dual-link channels in Fig. 10(a) and Fig. 9(a), we also observe the decrease of the fading variation brought by the channel diversity. The dual-link BER in walking case is better than in the sit-stand case

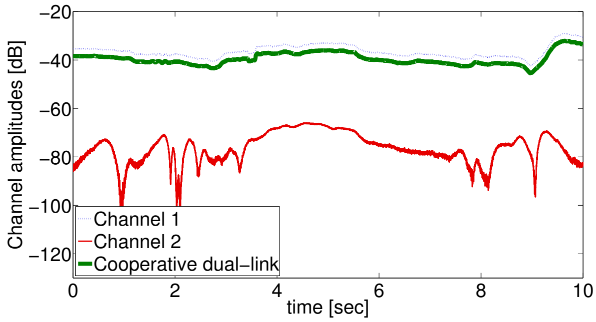

(a) Channel measurements

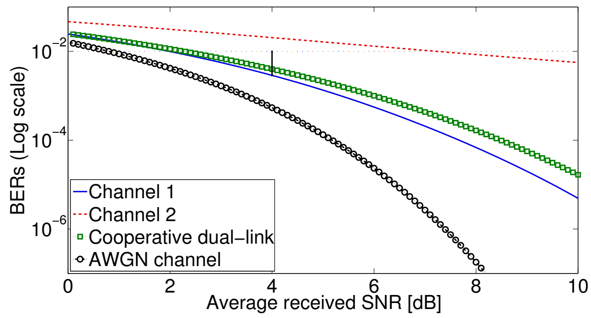

(b) BERs

Fig. 7. Effect of pathloss difference, scenario 1, sit-stand case

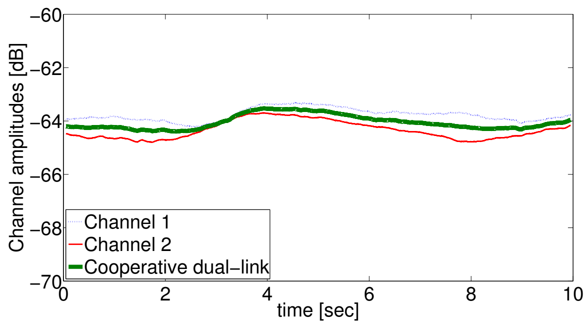

(a) Channel measurements

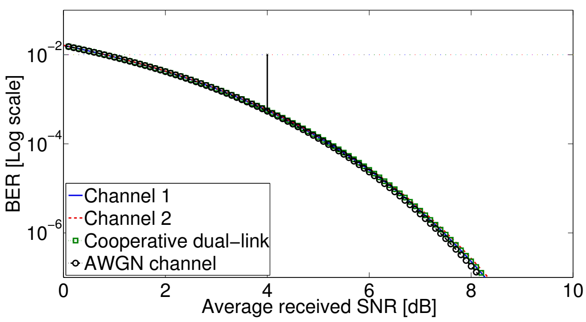

(b) BERs

Fig. 8. Effect of small channel fading, scenario 4, sleeping case

for two possible reasons: (1) the single links in the walking case are characterized by a smaller fading variance and (2) anti-correlation is found between the channels in the walking case.

The above analysis shows that the diversity gain obtained in a simple cooperation scheme, like the equal-power allocation simulated in the paper, is indeed jointly determined by the channel pathloss, fading, and correlation. In practical scenarios, the time and spatial variation of on-body channels could become quite large, especially when the body is changing the posture. Consequently, the performance of the cooperative on-body multi-links given specific link geometries is anticipated to encounter large fluctuation in different motion modes and environments.

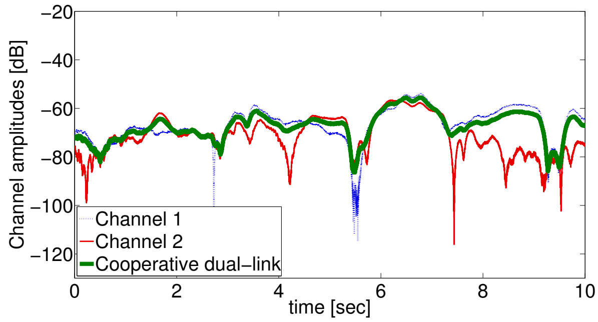

(a) Channel measurements

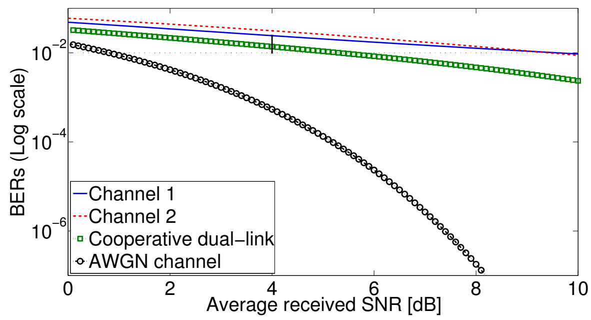

(b) BERs

Fig. 9. Channel measurements and diversity gain, scenario 2, sit-stand case

V. Conclusion

In this paper, we have evaluated the performance of a cooperative dual-link on-body communications using a simple equal-power allocation scheme based on channel measurements in typical indoor environments. Various link geometries and body movements have been investigated, which show significant differences with respect to the channel fading characteristics. Such differences are also reflected into the BER analysis when comparing single-link and dual-link schemes. The BER is able to exploit the channel spatial diversity if the involved single links fulfill the following conditions: (1) the channels in both single links exhibit close pathloss levels, (2) the variation of the channel fading is significant, (3) the channel correlation is low or negative. Spatial diversity is a key

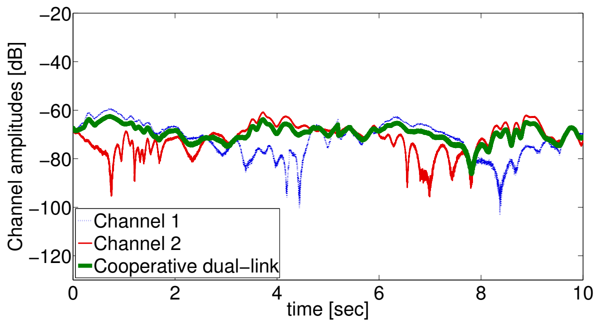

(a) Channel measurements

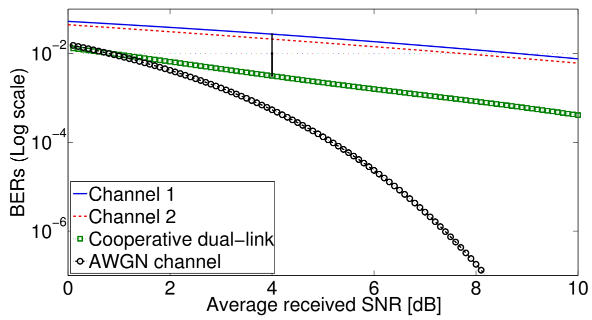

(b) BERs

Fig. 10. Channel measurements and diversity gain, scenario 2, walking case

factor for WBAN networks to mitigate the deep fading of on-body channels, and the reliability of WBAN communications can be effectively improved using cooperative multi-links, which is critical for biomedical data transmission in daily applications.

ACKNOWLEDGMENT

This work was funded by the Région Wallone in the framework of research contract 616449 *WALIBI* within the WIST-2 program. This work was also carried out in the framework of the COST 2100 Action. The authors would also like to thanks for the WELCOME facility of Université catholique de Louvain (UCL), Belgium, for the technical support provided during the measurements.

REFERENCES

[1] M. Kim and J.-I. Takada, "Statistical characterization of 4.5 ghz narrowband on-body propagation channel," *IEEE Antenna and Wireless Propagation Letters*, vol. 8, pp. 1250–1254, nov. 2009.

[2] S. C. Ergen, "ZigBee/IEEE 802.15.4 summary," Advanced Technology Lab of National Semiconductor, Tech. Rep., aug. 2004.

[3] E. Monton, J. Hernandez, J. Blasco, T. Herve, J. Micallef, I. Grech, A. Brincat, and V. Traver, "Body area network for wireless patient monitoring," *IET Communications*, vol. 2, no. 2, pp. 215 –222, feb. 2008.

[4] L. Liu, P. De Doncker, and C. Oestges, "Fading correlation measurement and modeling on the front side of a human body," in *Proc. 3rd EuCAP*, mar. 2009, pp. 969 –973.

[5] W. Scanlon and S. Cotton, "Understanding on-body fading channels at 2.45 ghz using measurements based on user state and environment," in *Proc. LAPC 2008. Loughborough*, mar. 2008, pp. 10–13.

[6] Y. Zhao, Y. Hao, A. Alomainy, and C. Parini, "Uwb on-body radio channel modeling using ray theory and subband fdtd method," *IEEE Trans. on Microwave Theory and Techniques,*, vol. 54, no. 4, pp. 1827 – 1835, jun. 2006.

[7] A. Sani, A. Alomainy, G. Palikaras, Y. Nechayev, Y. Hao, C. Parini, and P. Hall, "Experimental characterization of uwb on-body radio channel in indoor environment considering different antennas," *IEEE Trans. on Antennas and Propagation*, vol. 58, no. 1, pp. 238 –241, jan. 2010.

[8] Y. Chen, J. Teo, J. Lai, E. Gunawan, K. S. Low, C. B. Soh, and P. Rapajic, "Cooperative communications in ultra-wideband wireless body area networks: Channel modeling and system diversity analysis," *IEEE Journal on Selected Areas in Communications,*, vol. 27, no. 1, pp. 5–16, jan. 2009.

[9] R. D'Errico and L. Ouvry, "Time-variant ban channel characterization," in *Proc. IEEE 20th Int. Symp. on PIMRC*, sep. 2009, pp. 3000 –3004.

[10] J. G. Proakis, *Digital Communications*, 4th ed. McGraw-Hill Science/Engineering/Math, 2001.

[11] C. Oestges and B. Clerckx, *MIMO Wireless Communications: From Real-World Propagation to Space-Time Code Design*. Academic Press, 2007.

[12] D. Tse and P. Viswanath, *MIMO Wireless Communications: From Real-World Propagation to Space-Time Code Design*. Academic Press, 2007.

[13] S. Alamouti, "A simple transmit diversity technique for wireless communications," *IEEE Jour. on Selected Areas in Comm.*, vol. 16, no. 8, pp. 1451 –1458, oct 1998.

[14] W. Weichselberger and K. Hugl, "Optimum power allocation for transmit diversity in mobile communications," in *Proc. ICT 2003*, vol. 2, feb. 2003, pp. 1555–1560 vol.2.

[15] E. G. Larsson and P. Stoica, *Space-time block coding for wireless communications*. Cambridge Press, 2003.